XAI-Guided Enhancement of Vegetation Indices for Crop Mapping

Hiba Najjar[1,2], **Marlon Nuske**[2], **Andreas Dengel**[1,2]
[1]RPTU Kaiserslautern-Landau, Kaiserslautern, Germany
[2]German Research Center for Artificial Intelligence (DFKI), Kaiserslautern, Germany
najjar@rptu.de, marlon.nuske@dfki.de, andreas.dengel@dfki.de

Abstract

The global availability of satellite-derived vegetation indices allows to efficiently monitor vegetation growth and agricultural activities. Previous generations of satellites were capturing only a limited number of spectral bands, and a few expert-informed vegetation indices were sufficient to harness their potential. New generations of multi- and hyperspectral satellites can capture numerous additional spectral bands which are not yet efficiently exploited by traditional vegetation indices. In this work, we propose an explainable-AI-based framework to select and design suitable vegetation indices for a given downstream application task. The application chosen for this work is crop classification. Specifically, we train a deep network to predict crop types using 10 satellite bands from the Sentinel-2 mission, and use a feature attribution method to identify the most important bands for predicting each crop. We subsequently select suitable existing vegetation indices and, if needed, modify them to incorporate the identified bands. We validate our approach by training lightweight models using different vegetation indices and comparing their performance. Our results indicate that models trained on individual indices achieve comparable results to the baseline model trained on all bands. Furthermore, the combination of two indices surpasses the baseline in certain cases, exhibiting a 3 percentage point improvement in overall accuracy. Additionally, this combined approach demonstrates a more substantial advantage for individual crop types.

Introduction

Agricultural activities are a central focus of international efforts aimed at addressing the zero hunger sustainable development goal (Leal Filho et al. 2020). Efficiently managing natural and human resources in regions suffering from food insecurity and malnutrition is essential to improve both nutritional and economic well-being. Ground surveys and in-situ monitoring of agricultural activities, however, present challenges due to their elevated cost and restricted spatial coverage, urging the prioritization of alternative approaches. Crop type mapping, in particular, plays a crucial role in downstream tasks such as the monitoring of crop health, the estimation of yields, understanding the distribution of cultivated crops, and identifying gaps concerning population demand.

XAI4Sci: Explainable machine learning for sciences, AAAI-24 (xai4sci.github.io)

Meanwhile, there has been a notable surge in satellite data availability in recent years, holding promising potential for agricultural monitoring. Specifically, satellite data, with its global coverage and high temporal resolution, can be harnessed for tasks such as identifying cultivated lands, delineating fields, mapping crop types, and estimating seeding and harvesting dates, among other agriculture-related tasks.

In recent years, an increasing number of studies have employed Machine Learning (ML) and Deep Learning (DL) techniques to harness remote sensing data for addressing sustainable development goals (Ferreira, Iten, and Silva 2020). While such models are proficient in processing raw satellite bands, a common data engineering practice in this field involves the utilization of vegetation indices (VIs). Ratios, differences, and derivatives between reflectance values from different spectral wavelengths can enhance the spectral signals associated with vegetation characteristics of interest, given that the original measurements of spectral reflectance constitute a mixed signal comprising vegetation canopies, shadows, soils, and other components present on the land surface (Zeng et al. 2022). While some VIs, such as the normalized difference vegetation index (NDVI) (Rouse et al. 1974), the enhanced vegetation index (EVI) (Huete et al. 2002), the soil-adjusted vegetation index (SAVI) (Huete 1988), are commonly used for crop monitoring, the selection of the most suitable vegetation index is not always straightforward (Zeng et al. 2022). Instead, the initial step involves identifying the sensitive wavelengths and corresponding VIs for their optimal utilization.

An advantage of using DL lies in the model's inherent capability to automatically extract crop-related features and discern interactions between raw bands. To extract scientific insights encoded in the model, eXplainable AI (XAI) techniques can uncover the inner workings of the model, facilitating an understanding of how individual satellite bands contribute to its predictions (Ras et al. 2022). Regarding the Sentinel-2 (S2) multispectral instruments in particular, they stand out as one of the few remote sensors with the capacity to capture red-edge (RE) wavelengths between 700 and 800nm. Notably, the additional RE bands remain underexplored for their potential to enhance crop classification through vegetation indices (Misra, Cawkwell, and Wingler 2020). Furthermore, short-wave infrared (SWIR) bands, typically used for water monitoring, have also received little attention in exploring their efficacy to track vegetation cover and its phenology (Misra, Cawkwell, and Wingler 2020). While some work have already used explainability techniques to identify important bands and time steps for crop classification based on satellite data (Campos-Taberner et al. 2020; Orynbaikyzy et al. 2020; Xu et al. 2021), none has exploited this analysis to guide through over a hundred VIs available in the literature (Xue and Su 2017). In this paper, we introduce an approach that leverages explainability methods to identify relevant bands and improve the use of VIs for crop mapping. The implementation of our approach can be accessed at https://github.com/DFKI-Earth-And-Space-Applications/XAI4CM_XAI4Sci_AAAI2024.

Methodology

Crop Dataset

In Sub-Suharan Africa, extreme food insecurity and malnutrition are prevalent in multiple countries. In this study, we leverage S2 data from Ghana and South Sudan to address this task. The datasets were initially published following their utilization in a semantic segmentation task by Rustowicz et al. (2019). The original data contains satellite image time series captured between January and December 2016 at a 10m resolution, and is labeled with multiple land cover classes. For our study, we merge the two datasets and retain only the pixels corresponding to crops. We focus our work on classes with more than 10,000 labeled pixels: sorghum, maize, rice, groundnut, soybean, and yam. Table 1 presents the data distribution in each country. We partition 5% of the data for validation, ensuring that pixels originating from the same satellite image patch are exclusively utilized for either training or validation but not both.

Table 1: Pixel count per crop type.

Crop	Total	Ghana	S-Sudan
Maize	329.847	322.767	7.080
Groundnut	101.314	96.371	4.943
Rice	98.986	93.908	5.078
Soybean	67.638	67.638	-
Sorghum	65.185	8.352	56.833
Yam	22.091	22.091	-

Exploiting spectral attributions

Feature attribution methods are explanation techniques that provide interpretations for individual predictions. These methods assign sensitivity or contribution scores to each input feature, quantifying their relative importance to the model's prediction (Lundberg and Lee 2017). In our experiments, we use the Shapley Value Sampling (SVS) to estimate feature attributions (Strumbelj and Kononenko 2010). SVS is grounded in cooperative game theory, which provides a solid theoretical foundation, unlike many other methods (Lundberg and Lee 2017). Its robustness has being quantitatively evaluated in the context of a regression task based on time series of satellite data, and has shown superior stability against several other techniques (Najjar et al. 2023).

The results of the spectral attribution are used to improve the selection of VIs for the crop mapping task. We explain the model trained on multiple bands from the satellite data to identify the important bands. Subsequently, we use this information to select VIs that account for these bands, and adjust existing indices as needed. The model is then retrained by replacing the satellite bands with the individual indices or binary combinations, followed by a re-evaluation of the model on the validation set.

Experimental setup

We use ten bands from S2 data for our analysis, including blue (B02), green (B03), red (B04), three RE bands (B05, B06, B07), near-infrared (NIR) (B08), narrow near-infrared (n-NIR) (B8A), and two SWIR (B11, B12) bands. An additional channel, indicating the cloud coverage of the image, is stacked to these bands and used in all our experiments.

Regarding the modeling, we rely on recurrent neural networks, which have successfully been used to analyze temporal satellite data (Jia et al. 2017; Sharma, Liu, and Yang 2018; Garnot et al. 2019; Mou, Bruzzone, and Zhu 2018). We opt for the Gated Recurrent Unit (GRU), introduced in (Chung et al. 2014), due to its moderate number of parameters and its proven effectiveness in remote sensing applications (Garnot et al. 2019; Interdonato et al. 2019; Mou, Ghamisi, and Zhu 2017). The time series of each pixel are pre-padded to a fixed sequence length of 228, to account for the longest time series in the dataset, before being supplied to the model pixel-wise.

To handle the unbalanced labels in the data, we use a weighted sampler during training. This sampler assigns higher probabilities to small classes over large classes, enabling the model to train on a similar number of samples from each class during each training epoch.

Results

Spectral attributions

We train the GRU-based model using the satellite bands and present the evaluation results on the validation set in the second column of Table 2. This baseline model achieved a score of 67% on both the overall accuracy (OA) and F1 metrics. In individual classes, high accuracies of 84% and 86% were attained for rice and sorghum, respectively, while yam exhibited the lowest score at 27%. This could be attributed to the relatively small number of pixels in this class. Notably, the largest two classes did not necessarily exhibit the best performance, suggesting that the performance gaps are not solely due to the size of each class.

We interpret the baseline model following the procedure described in the previous section, and visualize the corresponding results in Figure 1. Starting with the global average attribution line, SWIR1 and RE1 rank at the top with around 20% of the total importance, followed by the red, SWIR2, n-NIR, and NIR bands, in the descendant order of their respective importance. The remaining bands exhibit a less significant importance. Notably, the relatively small importance of the cloud mask across all classes indicates that

Table 2: Experimental results of all trained models. The best score in each experimental group is in bold.

	S2	Single VI							Two VIs						
S2	x	—	—	—	—	—	—	—	—	—	—	—	—	—	—
NDVI	—	x	—	—	—	—	—	—	x	x	x	—	—	—	—
nNDVI	—	—	x	—	—	—	—	—	—	—	—	—	—	x	x
NDRE	—	—	—	x	—	—	—	—	x	—	—	x	x	x	—
NDRE2	—	—	—	—	x	—	—	—	—	x	—	—	—	—	—
NDRE3	—	—	—	—	—	x	—	—	—	—	x	—	—	—	—
NDMI	—	—	—	—	—	—	x	—	—	—	—	x	—	—	x
NDMI2	—	—	—	—	—	—	—	x	—	—	—	—	x	—	—
OA	0.67	0.62	0.62	0.61	0.56	0.51	**0.65**	0.63	0.64	0.62	0.62	0.67	**0.70**	0.61	0.68
F1	0.67	0.63	0.62	0.61	0.57	0.52	**0.65**	0.64	0.65	0.62	0.63	0.67	**0.70**	0.62	0.69
Maize	0.65	**0.66**	0.61	0.65	0.54	0.41	0.62	0.60	0.67	0.60	0.61	0.63	**0.70**	0.61	0.66
Groundnut	0.51	0.45	0.51	0.48	0.45	0.44	**0.57**	0.50	0.49	0.51	0.57	**0.69**	0.61	0.44	0.61
Rice	0.84	0.64	0.70	0.62	0.62	0.64	0.73	**0.76**	0.66	0.74	0.66	0.77	**0.83**	0.71	0.81
Soybean	0.48	0.49	0.42	0.34	0.38	0.49	0.41	**0.50**	**0.50**	0.37	0.42	0.35	0.38	0.43	0.49
Sorghum	0.86	0.84	0.84	0.81	0.84	0.83	**0.87**	0.86	0.85	0.83	0.82	0.85	**0.88**	0.82	0.87
Yam	0.27	0.23	0.21	0.23	0.29	0.34	**0.38**	0.27	0.22	0.30	0.23	0.31	0.32	**0.33**	0.23

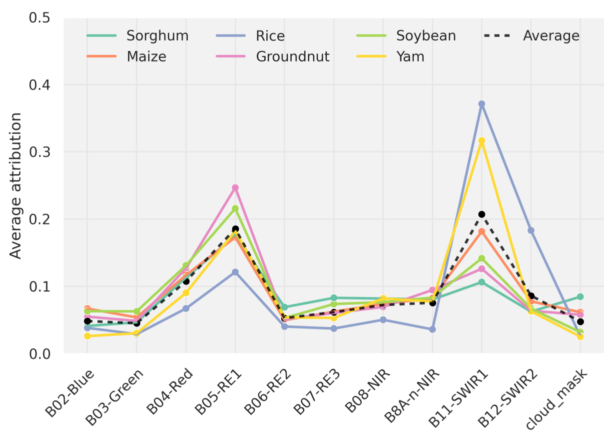

Figure 1: Global and crop-specific spectral attributions of the model trained on the ten satellite bands.

the model is not biased by this channel for the identification of any specific crop.

Analyzing the attribution results crop-wise, groundnut and soybean highly rely on the first RE band, followed by the red and SWIR1 bands. Sorghum has a similar attribution pattern. Rice has an additional particular dependence on the SWIR2 band. Rice and yam identification significantly rely on the first SWIR band, followed by RE1. All the remaining bands have each less than 10% of the total importance. Maize crop classification is sensitive to the first SWIR and RE bands, followed by the red band.

These results highlight the relevance of RE1 and SWIR1 bands for crop mapping and complement the findings of earlier studies. Yi, Jia, and Chen (2020) assessed the importance of S2 bands on the same task and found that RE1 and SWIR1 bands are more efficient in identifying crops than other bands in the Shiyang River Basin in China. Similarly, Liu, Qian, and Yue (2021) found that RE and SWIR bands of S2 had irreplaceable effects on land cover classification. Finally, the red band is sensitive to absorbing chlorophyll and the leaves absorb relatively more red than infrared light. This explains the relatively higher importance of the red band and its usage in the earliest VIs (Jordan 1969; Richardson and Wiegand 1977; Xue and Su 2017)

Table 3: VIs used for crop mapping. R, N, nN, S1, and S2 are the red, NIR, n-NIR, SWIR1, and SWIR2, respectively.

VI	Formula	Reference
NDVI	(N - R)/(N + R)	Rouse et al.
n-NDVI	(nN - R)/(nN + R)	This paper
NDRE	(N - RE1) / (N + RE1)	Gitelson and Merzlyak
NDRE2	(N - RE2) / (N + RE2)	This paper
NDRE3	(N - RE3) / (N + RE3)	This paper
NDMI	(N - S1)/(N + S1)	Wilson and Sader
NDMI2	(N - S2)/(N + S2)	This paper

Enhanced usage of VIs

In light of the insights gained from the importance of the satellite bands for crop mapping, we proceed with a guided selection of individual and binary combinations of VIs.

Given the significance of RE1, we include the normalized difference red edge (NDRE) (Gitelson and Merzlyak 1994) index that uses the NIR and RE1 bands. We derive two modified indices, NDRE2 and NDRE3, by replacing the first RE channel with the second and third, respectively, to verify whether the relative performance of the three indices align with the attribution of their respective bands. We also incorporate the normalized difference water index (NDMI), which uses the first SWIR band, and create a modified version, NDMI2, which uses the second SWIR band, influential on rice identification. Additionally, we include the widely used NDVI, and recognizing the comparable importance of n-NIR, we introduce a modified index, narrow normalized difference vegetation index (n-NDVI), where the NIR band is replaced with n-NIR.

It is important to note that only the red, green, blue, and NIR bands have a resolution of 10m, while the remaining bands were originally captured either at a 20 or 60m resolution. Therefore, we ensured that all our proposed indices contain at least one of the high-resolution bands. The formula of each index is listed in Table 3. We retrain our model using individual indices or combinations of two indices as inputs. The results are reported in Table 2.

Among the models trained on a single VI, the top-performing model is based on NDMI, achieving an OA score of 65%. This model outperformed the baseline in identifying three crops: sorghum, groundnut, and yam. The second-best model is based on the modified version of the same index, NDMI2, which achieved the same class accuracy as the baseline in sorghum and yam, and performed better in soybean. The third-best model, based on the NDVI, slightly outperformed the baseline on maize and soybean crops. The n-NDVI The NDRE3-based model achieved the lowest OA score, mainly due to its low accuracy in maize and rice crops.

Among the models trained on two VIs, the combination of NDRE and NDMI2 achieved the highest accuracies for sorghum, maize, and rice, and outperformed the baseline in groundnut and yam crops. This combination also scored an OA of 70%, 3 percentage points (p.p) higher than the baseline model. The combination of NDMI and n-NDVI also demonstrated comparable performance. In contrast, combining NDRE and n-NDVI had the worst overall performance, mainly due to its low accuracy in rice crops, despite its higher capacity to identify yam compared to the other models. The combinations of NDVI+NDRE2 and NDVI+NDRE3 also displayed comparatively low overall performance.

Discussion

Our overall approach of exchanging the raw satellite bands with few VIs exhibits promising results. The best model based on a single index exhibited an OA 2p.p lower than the baseline model, while using two indices achieved a 3p.p higher accuracy in the best case. These results highlight the potential of relying solely on one or two VIs for crop identification, especially when carefully selected. In general, larger datasets benefit from increased input features, as they enable automatic learning of high-level features by the model. However, in medium-sized training datasets like ours, performance can be enhanced through careful input feature selection.

As shown in Figure 1, SWIR1 appears to be significantly important to identify rice and yam crops, accordingly the NDMI-based models achieves the best accuracy for yam and the second-best score for rice, among the single-index based models. Combining NDMI with a second index also achieved high accuracies for both crops. We further observe that the proposed NDMI2 achieved the best accuracies on rice compared to the other single-VI based models. Additionally, it demonstrated the highest accuracies on sorghum, maize, and rice when combined with NDRE, outperforming all VI-based models. On the other hand, the proposed NDRE2 and NDRE3 indices performed poorly on the OA both when used individually and when combined with NDVI, in contrast to NDRE, which achieved high scores, particularly when combined with NDMI or NDMI2. This observation aligns with the relative average importance of the three RE bands, as shown in Figure 1, suggesting that the first band is more suitable for crop identification. Nonetheless, the second and third RE bands were of higher importance for soybean and sorghum compared to the remaining crops, which is consistent with the improvement in crop-specific accuracies achieved by the NDRE2 and NDRE3-based models compared to NDRE. In contrast, when combined with NDVI, the NDRE performs better in both crops.

While the performance of the VI-based modeling aligns with the attribution results conducted on the baseline model, there were some behaviors that were not easily interpretable. For instance, soybean identification relies significantly on the first RE band, and while RE1 and RE3 have marginal importance, according to the attribution results. Nonetheless, the soybean classification accuracy is the much worse when the model is trained with NDRE, compared to the NDRE2 and NDRE3 models. Similarly, the RE1 exhibits higher importance for identifying yam crop compared to the other two bands, while the performance of the three corresponding single- based models had the opposite behavior.

Overall, one limitation of our XAI-based approach is the reliability of the model. Meaningful explanation results and relevant scientific insights are conditioned by the scientific accuracy of what the model has learned during the training. Since our baseline had an OA score of 67%, we believe that further improvements in the model's performance can enhance its robustness, and consequently, the reliability of its attribution results.

In future work, in addition to improving the performance of the baseline model, we aim to extend the dataset to cover other regions from multiple years, and validate our approach on a broader range of crop types.

Conclusion

In this paper, we have successfully identified key VIs crucial for discerning various crop types, guided by the spectral importance results derived from the baseline model. Our research contributes significantly to the accumulating evidence highlighting the important role of information within the RE and SWIR bands from S2 imagery in discriminating crop types. Leveraging these insights, we trained multiple models using individual VIs and combinations of two, showing their ability to outperform the model trained on all spectral bands. Notably, the efficacy of these models aligned with the spectral importance in crop accuracies across most cases.

In summary, our work presents a comprehensive framework guiding practitioners through the vast array of over a hundred VIs documented in the literature. Beyond its application in crop type identification, our approach holds promise for broader applications in remote sensing such as forest health assessment, drought monitoring, soil moisture estimation and flood mapping.

Acknowledgments

H.Najjar acknowledges support through a scholarship from the University of Kaiserslautern-Landau. The authors also express their gratitude to the anonymous reviewers for their invaluable feedback and constructive comments, which contributed to the improvement of this manuscript.

References

Campos-Taberner, M.; García-Haro, F. J.; Martínez, B.; Izquierdo-Verdiguier, E.; Atzberger, C.; Camps-Valls, G.; and Gilabert, M. A. 2020. Understanding deep learning in land use classification based on Sentinel-2 time series. *Scientific reports*, 10(1): 17188.

Chung, J.; Gulcehre, C.; Cho, K.; and Bengio, Y. 2014. Empirical Evaluation of Gated Recurrent Neural Networks on Sequence Modeling. *arXiv preprint arXiv:1412.3555*.

Ferreira, B.; Iten, M.; and Silva, R. G. 2020. Monitoring sustainable development by means of earth observation data and machine learning: A review. *Environmental Sciences Europe*, 32(1): 1–17.

Garnot, V. S. F.; Landrieu, L.; Giordano, S.; and Chehata, N. 2019. Time-Space Tradeoff in Deep Learning Models for Crop Classification on Satellite Multi-Spectral Image Time Series. In *IGARSS 2019-2019 IEEE International Geoscience and Remote Sensing Symposium*, 6247–6250. IEEE.

Gitelson, A.; and Merzlyak, M. N. 1994. Quantitative estimation of chlorophyll-a using reflectance spectra: Experiments with autumn chestnut and maple leaves. *Journal of Photochemistry and Photobiology B: Biology*, 22(3): 247–252.

Huete, A.; Didan, K.; Miura, T.; Rodriguez, E. P.; Gao, X.; and Ferreira, L. G. 2002. Overview of the radiometric and biophysical performance of the MODIS vegetation indices. *Remote sensing of environment*, 83(1-2): 195–213.

Huete, A. R. 1988. A soil-adjusted vegetation index (SAVI). *Remote sensing of environment*, 25(3): 295–309.

Interdonato, R.; Ienco, D.; Gaetano, R.; and Ose, K. 2019. DuPLO: A DUal view Point deep Learning architecture for time series classificatiOn. *ISPRS journal of photogrammetry and remote sensing*, 149: 91–104.

Jia, X.; Khandelwal, A.; Nayak, G.; Gerber, J.; Carlson, K.; West, P.; and Kumar, V. 2017. Incremental Dual-memory LSTM in Land Cover Prediction. In *Proceedings of the 23rd ACM SIGKDD international conference on knowledge discovery and data mining*, 867–876.

Jordan, C. F. 1969. Derivation of leaf-area index from quality of light on the forest floor. *Ecology*, 50(4): 663–666.

Leal Filho, W.; Azul, A. M.; Brandli, L.; Özuyar, P. G.; and Wall, T. 2020. *Zero hunger*. Springer.

Liu, Y.; Qian, J.; and Yue, H. 2021. Comprehensive evaluation of Sentinel-2 red edge and shortwave-infrared bands to estimate soil moisture. *IEEE Journal of Selected Topics in Applied Earth Observations and Remote Sensing*, 14: 7448–7465.

Lundberg, S. M.; and Lee, S.-I. 2017. A unified approach to interpreting model predictions. *Advances in neural information processing systems*, 30.

Misra, G.; Cawkwell, F.; and Wingler, A. 2020. Status of phenological research using Sentinel-2 data: A review. *Remote Sensing*, 12(17): 2760.

Mou, L.; Bruzzone, L.; and Zhu, X. X. 2018. Learning Spectral-Spatial-Temporal Features via a Recurrent Convolutional Neural Network for Change Detection in Multispectral Imagery. *IEEE Transactions on Geoscience and Remote Sensing*, 57(2): 924–935.

Mou, L.; Ghamisi, P.; and Zhu, X. X. 2017. Deep Recurrent Neural Networks for Hyperspectral Image Classification. *IEEE Transactions on Geoscience and Remote Sensing*, 55(7): 3639–3655.

Najjar, H.; Helber, P.; Bischke, B.; Habelitz, P.; Sanchez, C.; Mena, F.; Miranda, M.; Pathak, D.; Siddamsetty, J.; Arenas, D.; Vollmer, M.; Charfuelan, M.; Nuske, M.; and Dengel, A. 2023. Feature Attribution Methods For Multivariate Time-Series Explainability In Remote Sensing. In *IGARSS 2023 - 2023 IEEE International Geoscience and Remote Sensing Symposium*.

Orynbaikyzy, A.; Gessner, U.; Mack, B.; and Conrad, C. 2020. Crop type classification using fusion of sentinel-1 and sentinel-2 data: Assessing the impact of feature selection, optical data availability, and parcel sizes on the accuracies. *Remote sensing*, 12(17): 2779.

Ras, G.; Xie, N.; Van Gerven, M.; and Doran, D. 2022. Explainable deep learning: A field guide for the uninitiated. *Journal of Artificial Intelligence Research*, 73: 329–396.

Richardson, A. J.; and Wiegand, C. 1977. Distinguishing vegetation from soil background information. *Photogrammetric engineering and remote sensing*, 43(12): 1541–1552.

Rouse, J. W.; Haas, R. H.; Schell, J. A.; and Deering, D. W. 1974. Monitoring vegetation systems in the Great Plains with ERTS. *NASA Spec. Publ*, 351(1): 309.

Rustowicz, R.; Cheong, R.; Wang, L.; Ermon, S.; Burke, M.; and Lobell, D. 2019. Semantic Segmentation of Crop Type in Africa: A Novel Dataset and Analysis of Deep Learning Methods. In *Proceedings of the IEEE/CVF Conference on Computer Vision and Pattern Recognition Workshops*, 75–82.

Sharma, A.; Liu, X.; and Yang, X. 2018. Land cover classification from multi-temporal, multi-spectral remotely sensed imagery using patch-based recurrent neural networks. *Neural Networks*, 105: 346–355.

Strumbelj, E.; and Kononenko, I. 2010. An efficient explanation of individual classifications using game theory. *The Journal of Machine Learning Research*, 11: 1–18.

Wilson, E. H.; and Sader, S. A. 2002. Detection of forest harvest type using multiple dates of Landsat TM imagery. *Remote Sensing of Environment*, 80(3): 385–396.

Xu, J.; Yang, J.; Xiong, X.; Li, H.; Huang, J.; Ting, K.; Ying, Y.; and Lin, T. 2021. Towards interpreting multi-temporal deep learning models in crop mapping. *Remote Sensing of Environment*, 264: 112599.

Xue, J.; and Su, B. 2017. Significant remote sensing vegetation indices: A review of developments and applications. *Journal of sensors*, 2017.

Yi, Z.; Jia, L.; and Chen, Q. 2020. Crop classification using multi-temporal Sentinel-2 data in the Shiyang River Basin of China. *Remote Sensing*, 12(24): 4052.

Zeng, Y.; Hao, D.; Huete, A.; Dechant, B.; Berry, J.; Chen, J. M.; Joiner, J.; Frankenberg, C.; Bond-Lamberty, B.; Ryu, Y.; Xiao, J.; Asrar, G. R.; and Chen, M. 2022. Optical vegetation indices for monitoring terrestrial ecosystems globally. *Nature Reviews Earth & Environment*, 3(7): 477–493.